PID Control Design and H_∞ Loop Shaping Design of PI Controllers Based on Non-Convex Optimization

Panagopoulos, Helene; Åström, Karl Johan

1999

INTERNATIONAL JOURNAL OF ROBUST AND NONLINEAR CONTROL
Int. J. Robust Nonlinear Control 2000; **10**:1249–1261

PID control design and $\mathscr{H}_\infty$ loop shaping

Hélène Panagopoulos and Karl J. Åström*,†

Department of Automatic Control, Lund Institute of Technology, Box 118, S-221 00 Lund, Sweden

SUMMARY

This paper shows that traditional methods for design of PID controllers can be related to robust $\mathscr{H}_\infty$ control. In particular, it shows how the specifications in terms of maximum sensitivity and maximum complementary sensitivity are related to the weighted $\mathscr{H}_\infty$ norm introduced by Glover and McFarlane [5]. The paper also shows how to use the Vinnicombe metric to classify those classes of systems which can be stabilized by the presented design methods in Åström *et al* [3] and Panagopoulos *et al* [4]. Copyright © 2000 John Wiley & Sons, Ltd.

KEY WORDS: $\mathscr{H}_\infty$ controller design; PID controller design; specifications; robustness

1. INTRODUCTION

In PID control it is attempted to control a complex process by using a controller with a simple, fixed structure. This differs from main stream control theory where no constraints are imposed on the controllers complexity. The problem of finding a controller of restricted complexity is often more complicated. For this reason, a number of specialized methods have been developed for PID control, see Reference [1]. In this paper it is attempted to show the similarities between some of the methods developed for PID control and main stream control theory which has also been done previously in Reference [2]. At the general level the problems are very similar because compromises between robustness and performances have to be dealt with. To mention a few differences between this paper and the one of Grimble [2] is that here we are not restricted to a special class of systems. Furthermore, for a given $\mathscr{H}_\infty$ norm the relations presented in this paper will give the corresponding PID controller which fulfills the specified robustness requirement.

The first aim of the paper is to show how the design methods for PI and PID controllers presented in References [3, 4] are related to the $\mathscr{H}_\infty$-loop-shaping method developed in References [5, 6].

Traditional design methods for PID controllers make a compromise between robustness and performance. For example, in Reference [7] the constraints on robustness and performance are

* Correspondence to: Karl Johan Åström, Department of Automatic Control, Lund Institute of Technology, Box 118, S-221 00 Lund, Sweden.
† E-mail: kja@control.lth.se

Received 6 October 1999
Revised 4 December 1999
Accepted 13 April 2000

expressed as, the Nyquist curve of the loop transfer function must lie outside a rectangle which encloses the critical point, and maximize the integral gain, respectively. The design methods for PI and PID controllers in References [3, 4] are based on this idea, but the robustness constraint is expressed as circles of constant sensitivity, constant complementary sensitivity or a combination of these two. Consequently, the robustness constraint of the proposed design methods can be viewed as a mixed sensitivity problem. In Reference [8] various aspects of the performance of linear single-input single-output feedback systems were translated into required bounds on the sensitivity function and its complement.

The idea of the $\mathscr{H}_\infty$-loop-shaping method is to design a controller which provides robustness to process uncertainties, and minimize the signal transmissions from load disturbance and measurement noise to process input and output. This can be expressed quantitatively by requiring the $\mathscr{H}_\infty$ norm, γ, of a 2×2 transfer function matrix to be small. The value of γ is then viewed as a design variable which determines the performance and robustness of the closed-loop system.

The paper shows how the condition that γ is small can be expressed in terms of requirements on the Nyquist curve of the loop transfer function. In particular, the curve should be outside a contour which encloses the critical point. An explicit formula is given for the contour of the region which can be bounded internally and externally by circles which are related to the maximum of the sensitivity function and the complementary sensitivity function. This establishes the relation between classical design conditions as in References [3, 4] to the one of $\mathscr{H}_\infty$ robust control. In Reference [9] a frequency interpretation of the $\mathscr{H}_\infty$ criteria is given where the sensitivity- and robustness-shaping techniques are formulated on Nyquist and Bode plots.

The second aim of the paper is to show how the previous relation between classical design conditions and the $\mathscr{H}_\infty$ robust control given in Reference [6] can be used to classify the class of systems which a PID controller will stabilize. In particular, it is shown how the specifications for the PID design in References [3, 4] should be chosen to guarantee that the weighted $\mathscr{H}_\infty$ norm of the transfer function from load disturbance and measurement noise to process input and output is less than a specified value γ. This problem has also been treated in Reference [10] where the results in Reference [6] have been used and the controller design is based on LQG.

2. $\mathscr{H}_\infty$ CONTROL

The design objectives of a typical process control problem are expressed as requirements on:

- Load disturbance response.
- Measurement noise response.
- Robustness with respect to model uncertainties.
- Set point response.

The first three design objectives are well captured by $\mathscr{H}_\infty$ loop shaping which makes it suitable for the design of process controllers, since they mostly operate as regulators. Set point weighting and filtering is then used to obtain a good set point response using the two-degrees-of-freedom structure proposed in Reference [11].

The $\mathscr{H}_\infty$ theory was originally developed by Zames [12] to emphasize plant uncertainties, but it is also well suited to treat the issues of load disturbance and measurement noise. Consider the block diagram in Figure 1 where the inputs are the load disturbance l and the measurement noise n. The outputs of interest are the process output x, and the signal v which represents the combined

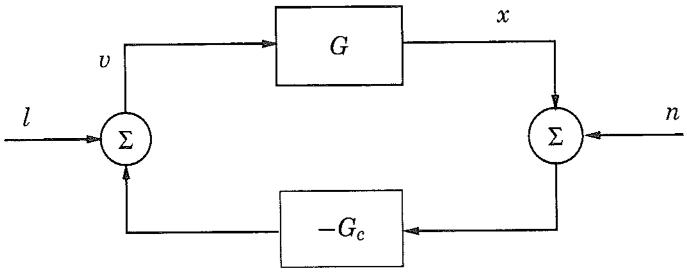

Figure 1. Block diagram describing the design problem of $\mathscr{H}_{\infty}$ control.

action of the load disturbance l and the control signal u. It is assumed that the controller G_c gives a stable closed-loop systems. The signals are related through

$$\begin{bmatrix} x \\ v \end{bmatrix} = H \begin{bmatrix} n \\ l \end{bmatrix}$$

where

$$H = \begin{bmatrix} G \\ I \end{bmatrix} (1 + GG_c)^{-1} [- G_c \; I] \tag{1}$$

The block diagonal elements in Equation (1) are the complementary sensitivity function

$$T = - G(I + GG_c)^{-1} G_c$$

and the sensitivity function

$$S = (I + GG_c)^{-1}$$

The off-diagonal elements are the transfer functions

$$G(I + GG_c)^{-1}$$
$$- (I + GG_c)^{-1} G_c$$

A good closed loop performance requires both x and v to be small with respect to the disturbances l and n which implies making the transfer function H small in the $\mathscr{H}_{\infty}$-norm, that is,

$$\gamma = \|H\|_{\infty} \tag{2}$$

should be small. The fact that γ is small will also guarantee the closed-loop system to be robust with respect to model uncertainties. Consequently, the $\mathscr{H}_{\infty}$ loop shaping is understood as minimizing the complementary sensitivity function T and the sensitivity function S indirectly rather than directly which is to be compared to the design methods for PI and PID controllers in Section 3.

The use of the parameter γ as a criterion for loop shaping was suggested by Glover and McFarlane [5] and McFarlane and Glover [13]. They recommended values of γ in the range [2, 10]. Furthermore, they showed that their design method had nice properties, such as:

- It gives a good controller if one exists.

- The obtained closed-loop system is stable against coprime factor uncertainties, [14]
- The parameter γ is a good design variable.

In the case of single-input single-output systems the transfer function H in (1) becomes

$$H = \frac{1}{1 + GG_c}\begin{bmatrix} -GG_c & G \\ -G_c & I \end{bmatrix} \tag{3}$$

The matrix H is of rank 1, and its largest singular value is given by

$$\sigma^2(H) = \frac{(1 + G_c G_c^*)(1 + GG^*)}{(1 + GG_c)(1 + G^* G_c^*)}$$

It follows from Equation (2) that

$$\gamma^2 = \sup_{\omega} \frac{(1 + G_c G_c^*)(1 + GG^*)}{(1 + GG_c)(1 + G^* G_c^*)} \tag{4}$$

3. PID CONTROL

Design methods for PI and PID controllers based on constraints of the maximum sensitivity and complementary sensitivity are described in References [3, 4]. A short review of the controller design is given in this section. The formulation of the design problem for the two methods coincide, they are therefore presented together.

The PID controller is described by the transfer function

$$G_c(s) = k + \frac{k_i}{s} + k_d s$$

where k is the controller gain, k_i is the integral gain, and k_d is the derivative gain. In reality, its structure is more complicated, because of the set point weight and filter, and the measurement noise filter, see Reference [4]. The problem formulation of the design methods are: Maximize the integral gain k_i subject to the robustness constraint that the Nyquist curve of the loop transfer function should lie outside a specified circle. This idea, which goes back to Reference [7] is discussed in detail in References [3, 4], where the robustness is measured in the classical terms of the maximum of the sensitivity function, M_s, and the maximum of the complementary sensitivity function, M_p. Thus, the robustness measure provides a transparent design variable which is expressed as

$$M_s = \|(1 + GG_c)^{-1}\|_\infty$$

that is, the Nyquist curve of the loop transfer function avoids the circle with centre at $C = -1$ and radius $R = 1/M_s$, compare with Figure 2, or

$$M_p = \|GG_c(1 + GG_c)^{-1}\|_\infty$$

that is, the Nyquist curve of the loop transfer function avoids the circle with centre at $C = -M_p^2/(M_p^2 - 1)$ and radius $R = |M_p/(M_p^2 - 1)|$, compare with Figure 2. It is possible to replace the constraints on M_s and M_p with a combined one which reduces the computational effort substantially, see Reference [3]. For the combined constraint the Nyquist curve of the loop

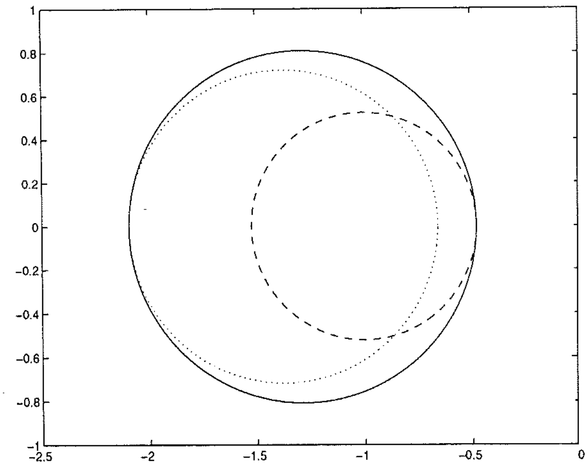

Figure 2. The M_s-circle (dashed line), the M_p-circle (dotted line) and the combined M_sM_p-circle (full line) for $M_s = M_p = 2.0$.

transfer function avoids the circle with centre at

$$C = -\frac{2M_sM_p - M_s - M_p + 1}{2M_s(M_p - 1)} \tag{5}$$

and radius at

$$R = \frac{M_s + M_p - 1}{2M_s(M_p - 1)} \tag{6}$$

see Figure 2. The circle will have its diameter on the interval $[-M_p/(M_p-1), -(M_s-1)/M_s]$. For practical purposes the constraint is not much more stringent than combining the two of M_s and M_p, respectively, but it is convex and will then be easier to handle computationally.

The combined constraint is simplified if both the sensitivity and the complementary sensitivity function are less than or equal to M, that is the Nyquist curve of the loop transfer function avoids the circle with centre

$$C = -\frac{2M^2 - 2M + 1}{2M(\mathrm{M} - 1)}$$

and radius

$$R = \frac{2M - 1}{2M(M - 1)}$$

The circle will have its diameter on the interval

$$\left[-\frac{M}{(M-1)}, -\frac{(M-1)}{M}\right] \tag{7}$$

4. COMPARISONS

The $\mathscr{H}_\infty$ loop shaping cannot immediately be related to the classical robustness criteria such as the maximum sensitivity M_s and the maximum complementary sensitivity M_p as they only depend on the loop transfer function $L = GG_c$. For the design methods in References [3, 4] the controller complexity is fixed, and its low-frequency gain is optimized subject to a robustness constraint. It is expressed in terms of either the maximum of the sensitivity function M_s, or the maximum of the complementary sensitivity function M_p, or a combination of the two.

The $\mathscr{H}_\infty$ norm γ depends on both G_c and G but the sensitivities depend only on the combination GG_c. By scaling the system matrix H given by Equation (3) we will find that the $\mathscr{H}_\infty$ norm of the scaled matrix will depend only on GG_c thus making the comparison possible.

The $\mathscr{H}_\infty$ norm of H can be interpreted as the gain from the disturbances n and l to the outputs v and x. The norm implicitly assumes that both disturbances have the same magnitude. The scaling can be interpreted as scaling of the disturbances

$$\bar{l} = Wl$$

$$\bar{n} = W^{-1}n$$

The case of scaling disturbance l and its equivalent block diagram are shown in Figures 3 and 4, respectively. According to Figure 4 we introduce for the scaled process $G' = GW$ and for the scaled controller $G_c' = G_c W^{-1}$. The same relations hold if the noise n would be scaled as $\bar{n} = W^{-1}n$. Thus, the loop transfer function L is invariant to the scaling W, that is

$$L' = G'G_c' = GG_c = L$$

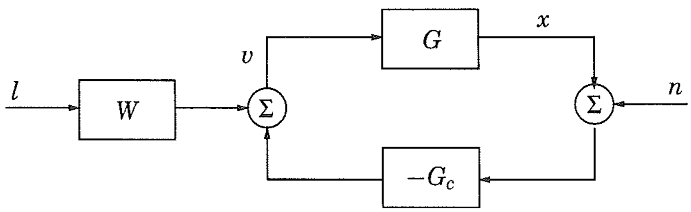

Figure 3. The scaling of the disturbance l with the weight W.

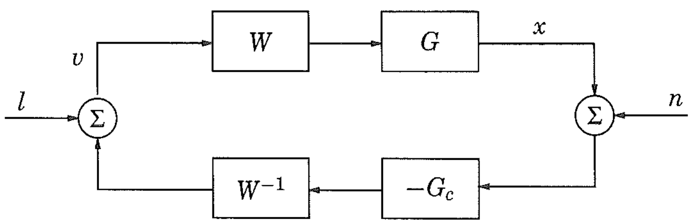

Figure 4. The equivalent block diagram of above.

Consequently, the transformed transfer function H in (3) becomes

$$\tilde{H} = \frac{1}{1 + GG_c}\begin{bmatrix} -GG_c & GW \\ -G_cW^{-1} & 1 \end{bmatrix} \tag{8}$$

and the robustness measure γ is given by

$$\gamma^2 = \sup_\omega \frac{(1 + G_cG_c^*W^{-1}W^{-1*})(1 + GG^*WW^*)}{(1 + GG_c)(1 + G^*G_c^*)} \tag{9}$$

A straightforward calculation shows that γ is minimized for the scaling

$$W = \sqrt{\frac{|G_c|}{|G|}} \tag{10}$$

Consequently, the scaling will typically enhance low and high frequencies.

Example 1 (*Determination of the scaling W*)

To illustrate the above result the following process is considered:

$$G(s) = \frac{1}{(s+1)^4} \tag{11}$$

A PI controller is designed using the design method in Reference [3] with the combined M-circle $M = 2.00$. The controller parameters are given by $k = 0.76$ and $k_i = 0.36$, for which the scaling W given in Equation (10) can be calculated. In Figure 5 the amplitude function of W is shown, which looks quite reasonable as it enhances the high and low frequencies. □

The determination of the scaling W in (10) makes it now possible to show how the specifications of the design methods for PI and PID controllers should be chosen to guarantee the $\mathscr{H}_\infty$ norm to be less than a specified value γ. By introducing (10) into (9) we find that γ is given by

$$\gamma^2 = \sup_\omega \frac{(1 + |GG_c|)^2}{|1 + GG_c|^2} \tag{12}$$

This implies that

$$\gamma = \max_\omega(|S(i\omega)| + |T(i\omega)|) \tag{13}$$

Consequently, Equation (13) shows that the robustness measure γ is related to the values M_s and M_p which are also used as robustness constraints for the design methods presented in Section 3. Notice that even if the scaling W in Equation (10) depends on the transfer functions G_c and G, the quantity γ depends only on the loop transfer function L. The robustness measure in Equation (12) is also found in the book by Doyle *et al.* [15].

Although the robustness measure of the $\mathscr{H}_\infty$ design, and the robustness constraint of the design methods for PI and PID controllers are related, there are some fundamental differences between the design methods. For example, in the $\mathscr{H}_\infty$ design the tuning parameter γ is insensitive to k_i for low frequencies, and the requirements on the transfer functions $G_c/(1 + GG_c)$ and $G/(1 + GG_c)$ appear explicitly in Equation (3). On the other hand, the design methods in Section 3 attempt to maximize k_i explicitly.

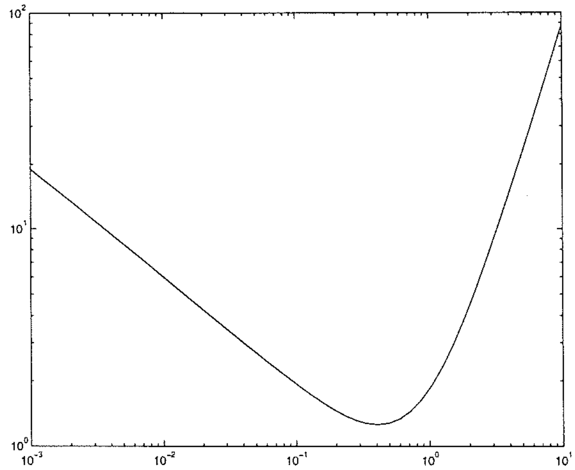

Figure 5. The amplitude function of the computed scaling W for the process $G(s) = 1/(s+1)^4$ with a PI controller $k = 0.76$ and $k_i = 0.36$.

4.1. *The gamma contour*

Below, a graphical interpretation of the robustness measure γ in Equation (12) will be given. Let $L = GG_c$ be the loop transfer function, then it follows from Equation (12) that

$$\gamma = \sup_{\omega} \frac{1 + |L|}{|1 + L|} \tag{14}$$

The condition $\gamma \leqslant \gamma_0$ implies that the Nyquist curve of the loop transfer function should lie outside the contour $(1 + |L|)/(|1 + L|)$. Therefore, it is suitable to continue the analysis in the complex plane. If $L = re^{i\varphi}$ is introduced, straightforward calculations of Equation (14) give the expression of the γ-contour, that is,

$$r(\varphi) = -\frac{\gamma^2 \cos\varphi - 1}{\gamma^2 - 1} \pm \sqrt{\left(\frac{\gamma^2 \cos\varphi - 1}{\gamma^2 - 1}\right)^2 - 1}$$

Typical contours for different values of γ are given in Figure 6.

4.2. *Relations between M and γ*

Figure 6 indicates that the γ-contours are close to circles at least for small values of γ. In this section we will explore the relations between M and γ further. We have

$$\gamma = \sup(|S| + |T|) \leqslant \sup|S| + \sup|T| = 2M$$

Furthermore

$$\gamma = \sup(|S| + |T|) \geqslant \sup(|S| + |S| - 1) = 2M - 1$$

Combining these two inequalities gives

$$2M - 1 \leqslant \gamma \leqslant 2M \tag{15}$$

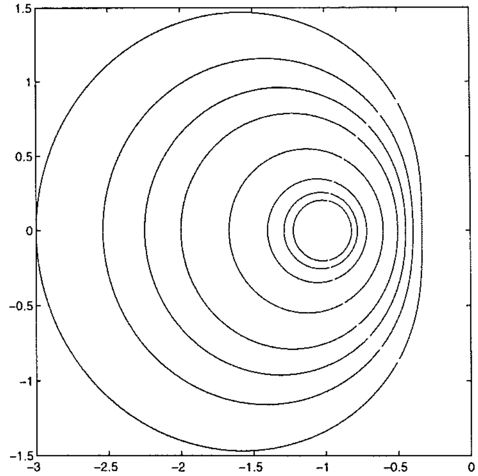

Figure 6. In the figure the loci of $(1+|L|)/(|1+L|)=\gamma$ for $\gamma=2$ (outer cave), 2.3, 2.6, 3, 4, 6, 8, 10 (inner curve) are shown.

We will now investigate how the γ-contours can be bounded by M-circles in the best way. The largest M-circle that is enclosed by a γ-curve will first be determined. To do so observe that the γ-contour intersects the negative real axis. The intersection points are given by putting $\varphi=-\pi$ in Equation (4) which gives us the intersection

$$x=\begin{cases} -(\gamma-1)/(\gamma+1) \\ -(\gamma+1)/(\gamma-1) \end{cases}$$

Matching these points of intersection with the ones of the M-circle gives

$$\frac{\gamma+1}{\gamma-1}=\frac{M}{M-1}$$

The largest M-circle which will enclose the γ-contour will have the M-value

$$M=\tfrac{1}{2}(1+\gamma) \tag{16}$$

Compare with inequality (15).

To find the smallest M-circle that encloses the γ-contour we first observe that for Equations (5) and (6),

$$C^2-R^2=1$$

holds this implies that the distance OA in Figure 7 is equal to 1. For a given γ-contour we will now take a M-circle that encloses it and shrink the M-circle until it touches the γ-contour. The M-circle will be parameterized by the angle that the line OA forms with the negative real axis. First observe that the tangent to the γ-curve which goes through the origin has a tangency for $r=1$ and $\cos\varphi=-1+2/\gamma^2$. Since both the M-circle and the γ-contour has a tangent going through the origin where tangency occurs at a distance 1 from the origin it will be easy to match the curves. Note that $\cos\varphi=-1+2/\gamma^2$ at the point of tangency then the distance between the

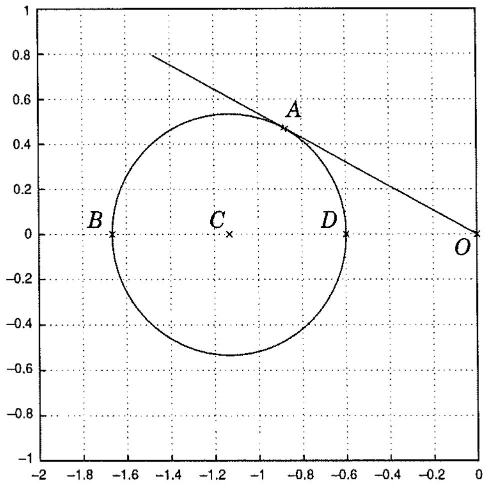

Figure 7. The following relations hold for the distances between the points in the figure: $OA = 1$, $OB = -(\gamma + 1/(\gamma - 1)$, $OC = \gamma^2/(2 - \gamma^2)$, $OD = -(\gamma - 1)/(\gamma + 1)$, $AC = 2((\gamma^2 - 1)/(\gamma^2 - 2)^2)^{1/2}$, $OB \cdot OD = 1$.

points O and C in Figure 7 will be $\gamma^2/(\gamma^2 - 2)$. If this distance is matched to the center of the M-circle in Equation (5) we find

$$\frac{2M^2 - 2M + 1}{2M(M-1)} = \frac{\gamma^2}{\gamma^2 - 2}$$

which can be simplified to

$$4M^2 - 2M + 2 = \gamma^2$$

Solving for M gives

$$M = \tfrac{1}{2}(1 + \sqrt{\gamma^2 - 1})$$

Summarizing we find that the γ-contour lies in the strip between M-circles corresponding to M_+ and M_- where

$$M_+ = \tfrac{1}{2}(1 + \sqrt{\gamma^2 - 1})$$
$$M_- = \tfrac{1}{2}(1 + \gamma)$$

Notice that the circles coincide as γ approaches infinity. Numerical values of γ, M_+ and M_- are given in Table I. The choice $M = 2.00$ guarantees a $\gamma < \sqrt{10}$ which gives good robustness according to Vinnicombe [6]. Lower values of M give even better robustness.

In Figure 8 the contours for constant γ, and the combined M-circles which encloses them are shown. Note how close the contours are for $\gamma = 3.16$ and $M = 2.00$. The figure indicates that the designs based on combined M-curves are not much more conservative than the one based on γ, particularly for $M = 2.00$. However, the calculations for constraint on γ are much more complicated.

Table I. Values of γ and M for circles that enclose (M_+) and are enclosed (M_-) by the γ-curve.

M_+	1.37	1.40	1.50	1.60	1.65	1.70	1.80	1.90	1.91	2.00
M_-	1.50	1.53	1.62	1.71	1.75	1.80	1.90	1.99	2.00	2.08
γ	2.00	2.06	2.24	2.42	2.50	2.60	2.79	2.97	3.00	3.16

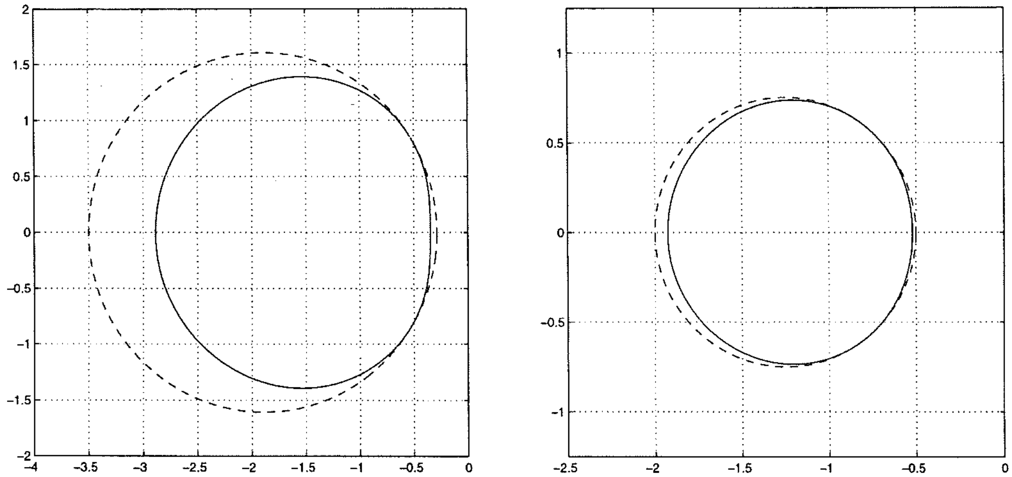

Figure 8. γ -curve (full line) for $\gamma = 2.06$ (left), 3.16 (right) enclosed by the combined M-circle (dashed line) for $M = 1.40$ (left), 2.00 (right).

5. CLASSIFICATION OF STABILIZABLE SYSTEMS

In Reference [6] much insight was given into the $\mathscr{H}_\infty$-loop-shaping procedure. He introduced the generalized stability margin b_{G,G_c} as a performance measure of the feedback system comprising the process G and the controller G_c defined as

$$b_{G,G_c} := \begin{cases} \dfrac{1}{\gamma} & \text{if } [G, G_c] \text{ is stable} \\ 0 & \text{otherwise} \end{cases}$$

where b_{G,G_c} lies in the range [0, 1]. Recall that γ was the $\mathscr{H}_\infty$ norm of the transfer function (1) that describes how the disturbances l and n propagate through the system. Consequently, a value of b_{G,G_c} which is close to 1 implies a controller with good disturbance attenuation. On the other hand, a value of b_{G,G_c} which is close to 0 implies a controller with poor disturbance attenuation. The solutions of many design examples, see References [6, 13], indicate that a value of $b_{G,G_c} > 1/\sqrt{10}$ or $\gamma < \sqrt{10}$ gives a reasonable robustness and performance, compare with the values in Table I.

In Reference [6] the ν-gap metric was introduced to measure the distance between two systems in terms of their frequency responses $G_1(\mathrm{i}\omega)$ and $G_2(\mathrm{i}\omega)$. For the scalar case it is defined as

$$\delta_\nu(G_1, G_2) := \sup_\omega \frac{|G_1(\mathrm{i}\omega) - G_2(\mathrm{i}\omega)|}{\sqrt{1 + |G_1(\mathrm{i}\omega)|^2}\sqrt{(1 + |G_2(\mathrm{i}\omega)|^2}}$$

subject to a winding number condition, see Reference [6]. Introduce the two scalar systems $G_1(s) = B_1(s)/A_1(s)$ and $G_2(s) = B_2(s)/A_2(s)$, which are not necessarily stable and where $A_j(s)$ and $B_j(s)$ are polynomials. The winding number condition will then be satisfied if

$$B_1(s)\, B_2(-s) + A_1(s)A_2(-s)$$

have the same number of roots as deg $A_2(-s)$ in the right half plane. If the winding condition is not satisfied then $\delta_\nu(G_1, G_2)$ is defined to be 1. Thus, the ν-gap metric, δ_ν, take values in the range [0, 1]. It is an important measure, since it means that the distance between two linear plants can be estimated directly from their frequency responses.

Vinnicombe has derived very interesting results relating the generalized stability margin to robustness and model uncertainty. He showed that if the closed-loop system (G, G_c) consisting of the controller G_c and the process G is stable with a generalized stability margin $b_{G,G_c} > \beta$, and $\bar{G}$ is a process which is "close" to G in the sense that $\delta_\nu(G, \bar{G}) \leqslant \beta$, then G_c is also guaranteed to stabilize $\bar{G}$.

A PID controller which is designed to satisfy the constraints $M_p < M_0$ and $M_s < M_0$ thus guarantees that $\gamma \leqslant \gamma(M_0)$. The results of Vinnicombe then gives a complete characterization of the class of systems which are stabilized by the controller.

Example 2 (*Classification of Stabilizable Systems*)

To illustrate the results above the process and controller in Example 1 are considered. The generalized stability margin for this design is $b_{G,G_c} = 0.32$. It is now possible to investigate the effects of model uncertainties. Assume, for example, that the true process is instead governed by the following model:

$$\bar{G}(s) = \frac{1}{(2s+1)^2}$$

To verify if the controller designed for the process G in Example 1, also works for $\bar{G}$, the ν-gap metric is calculated between G and $\bar{G}$, and compared to the generalized stability margin. The winding number condition of the ν-gap metric is fulfilled. Straightforward calculations gives that the largest values of $\delta_\nu(G, \bar{G})$ (≈ 0.25) is less than the smallest value of the generalized stability margin (≈ 0.32). Consequently, the controller designed for G will stabilize the system $\bar{G}$.

6. CONCLUSIONS

Traditional methods for designing PID controllers were related to robust $\mathscr{H}_\infty$ control, in particular the specifications of design methods for PI and PID controllers in References [3, 4] to the one of the weighted $\mathscr{H}_\infty$ norm in Reference [5], denoted γ. The requirement of a sufficiently small γ was expressed as, the Nyquist curve of the loop transfer function should lie outside a certain region. The region showed to be bounded internally and externally by circles closely related to the ones of constant sensitivity and constant complementary sensitivity, which is of use for efficient computations, see Reference [3]. Furthermore, it is shown how to use the Vinnicombe metric in Reference [6] to classify those classes of systems which can be stabilized by the presented design methods for PI and PID controllers in References [3, 4].

REFERENCES

1. Åström KJ, Hägglund T. *PID Controllers: Theory, Design, and Tuning*. Instrument Society of America: Research Triangle Park, NC, 1995.
2. Grimble MJ. '$\mathscr{H}_{\infty}$ controllers with a PID structure. *Transactions of the ASME Journal of Dynamic Systems, Measurement, and Control* 1990; **112**:325–336.
3. Åström KJ, Panagopoulos H, Hägglund T. Design of PI controllers based on non-convex optimization. *Automatica* 1998; **34**(5):585–601.
4. Panagopoulos H, Åström KJ, Hägglund T. Design of PID Controllers based on Constrained Optimization. In *1999 American Control Conference*, San Diego, CA 1999; 3858–3862.
5. Glover K, McFarlane D. Robust stabilization of normalized coprime factor plant descriptions with H_{∞}-bounded uncertainty. *IEEE Transactions on Automatic Control* 1989; **34**(8):821–830.
6. Vinnicombe G. *Uncertainty and Feedback. H_{∞} Loop-Shaping and the v-Gap Metric*. Imperial College Press; to be published.
7. Shinskey FG. How good are our controllers in absolute performance and robustness? *Measurement and Control* 1990; **23**:114–121.
8. Kwakernaak H. Minimax frequency domain performance and robustness optimization of linear feedback systems. *IEEE Transactions on Automatic Control* 1985; **10**(30):994–1004.
9. Bányász C, Keviczky L. Geometric tools to design robust control systems. In *IFAC'99, 14th World Congress of IFAC*, vol. G. Beijing, China, 1999; 277–282.
10. Bombois X, Gevers M, Scorletti G. Controller validation for a validated model set. In *European Control Conference'99*, Karlsruhe, Germany, 1999.
11. Horowitz IM. *Synthesis of Feedback Systems*. Academic Press: New York, 1963.
12. Zames G. Feedback and optimal sensitivity: model reference transformations, multiplicative seminorms and approximate inverses. *IEEE Transactions on Automatic Control* 1981; **AC-26**:301–320.
13. McFarlane D, Glover K. A loop shaping design procedure using H_{∞} synthesis. *IEEE Transactions on Automatic Control* 1992; **37**(6):759–769.
14. Vidyasagar M. *Control System Synthesis: A Factorization Approach*. MIT Press: Cambridge, MA, 1985.
15. Doyle JC, Francis BA, Tannenbaum AR. *Feedback Control Theory*. Macmillan Publishing Company: New York, 1992.

